論文 97-8-6-11

CDMA 시스템용 기저 대역 비동기식 동기 추적 회로의 성능 분석

Performance Analysis of a Baseband Noncoherent Code Tracking Loop for DS-CDMA Systems

이경준* · 박형래** · 채수환**

Kyoung-Joon Lee · Hyung-Rae Park · Soo-Hoan Chae

Abstract

In this paper, the performance of the noncoherent code tracking loop designed at baseband for CDMA applications is analyzed in detail and is confirmed by computer simulations. Analytical closed-form formula for jitter variance is derived for AWGN channel environments as a function of pulse shaping filter, timing offset, signal-to-interference ratio, and loop filter coefficients. The design issue of the loop filter is also addressed with emphasis on the second-order tracking loop. Finally, the performance of the designed tracking loop is examined by computer simulations for both AWGN and Rayleigh fading channels, when applied to the reverse link of the coherent CDMA system for IMT-2000 designed by ETRI.

요 약

본 논문에서는 CDMA 시스템에 적용하기 위해 기저 대역에서 설계된 비동기식 동기 추적 회로의 성능을 이론적으로 분석하고 컴퓨터 시뮬레이션을 통해 검증한다. AWGN 채널 환경에서 지터 분산을 펄스 성형 필터, 타이밍 오프셋, 신호 대 잡음 비, 루우프 필터 계수의 함수로 이론적으로 유도하고 2차 동기 추적 회로를 중심으로 루우프 필터의 설계에 관해 고찰한다. 끝으로, 설계된 동기 추적 회로를 ETRI에서 IMT-2000을 위해 설계한 동기식 CDMA 시스템의 역방향 링크에 적용하여 AWGN과 레일라이 페이딩 환경에서의 성능을 시뮬레이션을 통해 검증한다.

I. Introduction

Recently, code division multiple access(CDMA) technique has attracted much attention for radio access of cellular mobile or personal communication systems [1]-[4]. However, like other spread spectrum applications, its attractive features can be exploited only in case where the pseudo-noise(PN) sequences of the

* 한국전자통신연구원 이동통신연구단 이동통신망연구부(Mobile Network Dept., Mobile Telecomminication Div., ETRI)
** 한국전자통신연구원 이동통신연구단 이동통신기술연구부(Mobile Communication Research Dept., Mobile Telecommunication Div., ETRI)
*** 한국항공대학교 컴퓨터공학과(Computer Engineering Dept., Hankuk Aviation University)

· 논 문 번 호 : 970919-060
· 수정완료일자 : 1997년 11월 20일

code synchronization process consists of two steps, code acquisition(coarse alignment) and code tracking(fine alignment), of which the latter is dealt with in this paper.

Once receiver timing has been obtained within one PN chip time by code acquisition process, more accurate timing estimate should be made through code tracking process. In this paper, the performance of the baseband noncoherent code tracking loop designed for CDMA applications is analyzed in detail. Traditionally for spread spectrum applications, noncoherent code tracking loops have been designed and analyzed at IF band to avoid prior carrier synchronization[5]~[8]. However, such approaches are not desirable for CDMA systems where the signal-to-interference ratio at the input of the phase detector is very small. Contrary to traditional spread-spectrum systems, the receiver carrier frequency is coarsely synchronized with that of the received signal in CDMA systems so that noncoherent code tracking loops can be designed at baseband.

Most performance analyses so far have not taken into account the effect of the pulse shaping filter which is inevitable for band-limiting the signal spectrum in CDMA systems[5]~[8]. A closed-form formula for steady-state jitter variance is derived as a function of pulse shaping filter, timing offset (advance or retard time), and loop filter coefficients for AWGN channel environments. The design issue of the loop filter is also addressed with emphasis on the second-order code tracking loop. The performance of the designed tracking loop is evaluated for various design parameters and is confirmed by computer simulations for both AWGN and Rayleigh fading environments, when applied to the reverse link of the coherent CDMA system for IMT-2000 designed by ETRI[4].

The paper is organized as follows. Signal model and system description are given in section Ⅱ. Theoretical derivation of the steady-state jitter variance is made in section Ⅲ together with the design issue of the loop filter. In section Ⅳ, tracking performance evaluations are made for various design parameters, followed by concluding remarks in section Ⅴ.

Ⅱ. Signal Model and System Description

2-1 Signal Model and Demodulator Output Statistics

The transmitted signal which is modulated by dual-channel QPSK scheme with the pilot signal can be written as

$$\begin{aligned} s(t) = & \sqrt{E_{c,t}^{(i)}}\cos(2\pi f_c t)\sum_{m=-\infty}^{\infty} x_{I,m}\, a_{I,m}^{(i)} W_{1,m}\, h(t-mT_c) \\ & + \sqrt{E_{c,t}^{(i)}}\sin(2\pi f_c t)\sum_{m=-\infty}^{\infty} x_{Q,m}\, a_{Q,m}^{(i)} W_{1,m}\, h(t-mT_c) \\ & + \sqrt{E_{c,p}^{(i)}}\cos(2\pi f_c t)\sum_{m=-\infty}^{\infty} a_{I,m}^{(i)}\, h(t-mT_c) \\ & + \sqrt{E_{c,p}^{(i)}}\sin(2\pi f_c t)\sum_{m=-\infty}^{\infty} a_{Q,m}^{(i)}\, h(t-mT_c) \end{aligned} \tag{1}$$

where $E_{c,t}^{(i)}$ and $E_{c,p}^{(i)}$ are the traffic and pilot signal energies per PN chip of the ith user, respectively, and $h(t)$ is the impulse response of the pulse shaping filter. $x_{I,m}$ and $x_{Q,m}$ are the I and Q channel information sequences and f_c is the carrier frequency. $a_{I,m}^{(i)}$ and $a_{Q,m}^{(i)}$ are the I and Q channel PN sequences of the ith user, respectively, and $W_{1,m}$ is the Walsh sequence with index 1 for differentiating the pilot and traffic channels. The received signal at the base station under frequency non-selective fading environments is given by

$$r(t) = \sum_{k=1}^{Nu} \alpha_k \cos(2\pi f_c t+\varphi_k) \sum_{m=-\infty}^{\infty} \Big\{ \sqrt{E_{c,t}^{(k)}}\, x_{Im,k}\, a_{I,m}^{(k)} W_{1,m} + \sqrt{E_{c,p}^{(k)}}\, a_{I,m}^{(k)} \Big\} h(t-mT_c-\tau_{d,k}) + \sum_{k=1}^{Nu} \alpha_k \sin(2\pi f_c t+\varphi_k) \sum_{m=-\infty}^{\infty} \Big\{ \sqrt{E_{c,t}^{(k)}}\, x_{Qm,k}\, a_{Q,m}^{(k)} W_{1,m} + \sqrt{E_{c,p}^{(k)}}\, a_{Q,m}^{(k)} \Big\} h(t-mT_c-\tau_{d,k}) + n_I(t)\cos(2\pi f_c t) - n_Q(t)\sin(2\pi f_c t) \qquad (2)$$

where $n_I(t)$ and $n_Q(t)$ are narrowband Gaussian noise processes due to background(or thermal) noise with the same variance N_o. N_u is the number of users and $\tau_{d,k}$ is the delay of the kth user. α_k and φ_k are the signal envelope and phase, respectively. The signal envelope is not necessarily be Rayleigh-distributed due to power control effect. Fig. 1 depicts the block diagram for demodulating the ith user's pilot signal. In the figure, $H^*(f)$ is the Fourier transform of the impulse response of the matched filter with " $*$ " denoting conjugate operation. When there is a timing error τ, I and Q channel demodulator outputs can be modeled as[9],[10]

$$Y_I = \alpha N \sqrt{E_{c,p}}\, R(\tau)\cos\varphi + n_I,$$
$$Y_Q = \alpha N \sqrt{E_{c,p}}\, R(\tau)\sin\varphi + n_Q, \qquad (3)$$

where the user index i has been dropped for notational convenience. N is the number of

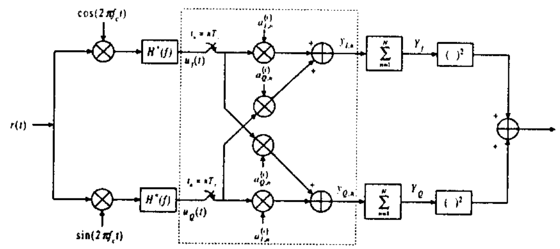

Fig. 1. Block diagram for demodulating the ith user's pilot signal.

accumulated PN chips and $R(t)$ is the convolution of the impulse responses of the pulse shaping filter and its matched filter, that is,

$$R(t) \equiv h(t) * h(-t) = \int_{-\infty}^{\infty} |H(f)|^2 \cos(2\pi f t)\, df. \qquad (4)$$

Without loss of generality, the pulse shaping filter can be normalized such that $R(0)=1$. n_I and n_Q are interferences due to background noise, inter-chip interference, and other-user signals, which can be modeled as Gaussian random variables independent of each other. The interference variance is given by[9],[10]

$$E[n_I^2] = E[n_Q^2] = NI_0/2 \qquad (5)$$

where I_o is the interference spectral density. In a CDMA reverse link, interference is due mainly to background noise and other-user signals such that the interference spectral density can be written as [10]

$$I_0 \approx N_0 \int_{-\infty}^{\infty} |H(f)|^2 df + \rho_o \cdot \frac{1}{T_c} \int_{-\infty}^{\infty} |H(f)|^4 df$$
$$= N_o + \rho_o \cdot \frac{1}{Tc} \int_{-\infty}^{\infty} |H(f)|^4 df$$

with

$$\rho_o = \sum_{\substack{k=1 \\ k \neq i}}^{N_u} \left\{ E_{c,p}^{(k)} + E_{c,t}^{(k)} \right\} \tag{7}$$

2-2 System Description

Fig. 2 depicts the baseband noncoherent code tracking loop. In the figure, y_{I-} and y_{Q-} (or y_{I+} and y_{Q+}) represent the I and Q channel outputs of the early(or late) sample processing unit. K_o and $\hat{\tau}$ are the VCO gain and the estimated timing error, respectively. The structure of the early or late sample processing unit is equivalent to the block drawn by dashed line in Fig. 1. The received signal is first down-converted to the baseband and then lowpass-filtered by the matched filter to maximize signal-to-interference ratio. I and Q channel baseband signals are over-sampled, in usual, four or eight times the PN chip rate. Early and late samples are used for generating the error signal ΔZ and correlation operations for them are done through the same I and Q channel PN generators used for data demodulation. After scaled by VCO gain, the error signal is lowpass-filtered by the loop filter

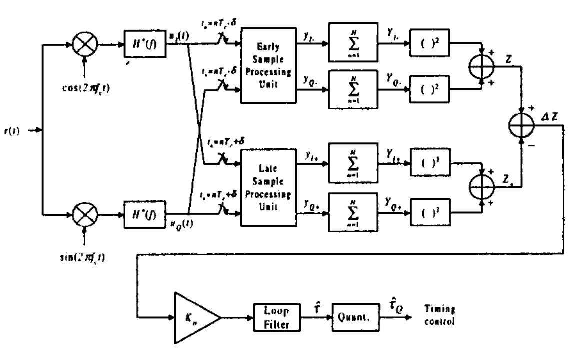

Fig. 2. Baseband noncoherent code tracking loop.

whose output corresponds to the timing error estimate. According to the timing error estimate, decimation points for the three sample sequences are updated.

Ⅲ. Performance Analysis

3-1 Phase Detector Output Statistics

Similarly to Eq. (3), we can model the early and late demodulator outputs under AWGN channel environments as follows,

$$Y_{I-} = N\sqrt{E_{c,p}}R(\tau-\delta)\cos\varphi + n_{I-},$$
$$Y_{Q-} = N\sqrt{E_{c,p}}R(\tau-\delta)\sin\varphi + n_{Q-} \tag{8}$$

and

$$Y_{I+} = N\sqrt{E_{c,p}}R(\tau+\delta)\cos\varphi + n_{I+},$$
$$Y_{Q+} = N\sqrt{E_{c,p}}R(\tau+\delta)\sin\varphi + n_{Q+} \tag{9}$$

with δ denoting the timing offset(advance or retard time). Therefore, we can obtain

$$Z_- \equiv Y_{I-}^2 + Y_{Q-}^2 = N^2 E_{c,p} R^2(\tau-\delta) + 2N\sqrt{E_{c,p}} R(\tau-\delta)(\cos\varphi \cdot n_{I-} + \sin\varphi \cdot n_{Q-}) + n_{I-}^2 + n_{Q-}^2 \tag{10}$$

and

$$Z_+ \equiv Y_{I+}^2 + Y_{Q+}^2 = N^2 E_{c,p} R^2(\tau+\delta) + 2N\sqrt{E_{c,p}} R(\tau+\delta)(\cos\varphi \cdot n_{I+} + \sin\varphi \cdot n_{Q+}) + n_{I+}^2 + n_{Q+}^2 \tag{11}$$

The mean of the phase detector output is given by

$$E[\Delta Z] \equiv E[Z_- + Z_+] = N^2 E_{cp}\{R^2(\tau-\delta) - R^2(\tau+\delta)\} \quad (12)$$

and the variance of ΔZ is

$$\mathrm{var}(\Delta Z) = E\Big[\{2N\sqrt{E_{cp}}R(\tau-\delta)(\cos\varphi \cdot n_{I-} + \sin\varphi \cdot n_{Q-}) - 2N\sqrt{E_{cp}}R(\tau+\delta)(\cos\varphi \cdot n_{I+} + \sin\varphi \cdot n_{Q+})\}^2\Big] + E\Big[(n_{I-}^2 + n_{Q+}^2 - n_{I+}^2 - n_{Q+}^2)^2\Big] \quad (13)$$

With some mathematical manipulation, we can obtain

$$\mathrm{var}(\Delta Z) = 4N^2 E_{cp} R^2(\tau-\delta) E[n_{I-}^2] + 4N^2 E_{cp} R^2(\tau+\delta) E[n_{I+}^2] - 8N^2 E_{cp} R(\tau-\delta) R(\tau+\delta) E[n_{I-} n_{I+}] + 4E[n_{I-}^4] - 4E[n_{I-}^2 n_{I+}^2] \quad (14)$$

Using the relationship, $E[x_1\ x_2\ x_3\ x_4] = E[x_1 x_2]\ E[x_3 x_4] + E[x_1 x_3]\ E[x_2 x_4] + E[x_1 x_4] E[x_2 x_3]$, for Gaussian random variables [12],[13], we can write

$$E[n_{I-}^4] = 3\{E[n_{I-}^2]\}^2 \quad (15)$$

and

$$E[n_{I-}^2\ n_{I+}^2] = \{E[n_{I-}^2]\}^2 + 2\{E[n_{I-} n_{I+}]\}^2 \quad (16)$$

It also follows from the interference statistics given by Eq. (6) that

$$E[n_{I-} n_{I+}] = \frac{N}{2}\{N_o\ R(2\delta) + \rho_o\ R_o(2\delta)\} \quad (17)$$

with

$$R_o(\tau) = \frac{1}{T_c}\int_{-\infty}^{\infty} |H(f)|^4 \cos(2\pi f\tau)\, df \quad (18)$$

Therefore,

$$\mathrm{var}(\Delta Z) = 2N^3 I_o E_{cp}\{R^2(\tau-\delta) + R^2(\tau+\delta)\} - 4N^3 E_{cp} R(\tau-\delta) R(\tau+\delta)\{N_o R(2\delta) + \rho_o\ R_o(2\delta)\} + 2N^2 I_o^2 - 2N^2\{N_o R(2\delta) + \rho_o\ R_o(2\delta)\}^2 \quad (19)$$

In most CDMA applications, the pulse shaping filter can be approximated by the ideal band-limiting filter with $H(f) = 1/\sqrt{W}$ for $-W/2 \le f \le W/2$ and $W = 1/T_c$. In this case, $R(\tau) = R_o\ (\tau) = \mathrm{sinc}(\tau/T_c)$ and thus the variance of ΔZ is given by

$$\mathrm{var}(\Delta Z) = 2N^2 I_o^2\{1 - R^2(2\delta)\} + 2N^3 I_o E_{cp} \{R^2(\tau-\delta) + R^2(\tau+\delta) - 2R(\tau-\delta) R(\tau+\delta) R(2\delta)\} \quad (20)$$

With an assumption that the timing error is very small, that is, $\tau \approx 0$, the variance becomes to

$$\mathrm{var}(\Delta Z) \approx 2N^2 I_o^2\{1 - R^2(2\delta)\} + 4N^3 I_o E_{cp} R^2(\delta)\{1 - R(2\delta)\} \quad (21)$$

3-2 Derivation of the Steady-State Jitter Variance

Define the error metric signal

$$G(\tau) \equiv R^2(\tau-\delta) - R^2(\tau+\delta) \quad (22)$$

Using the above equation, S-curve is depict-

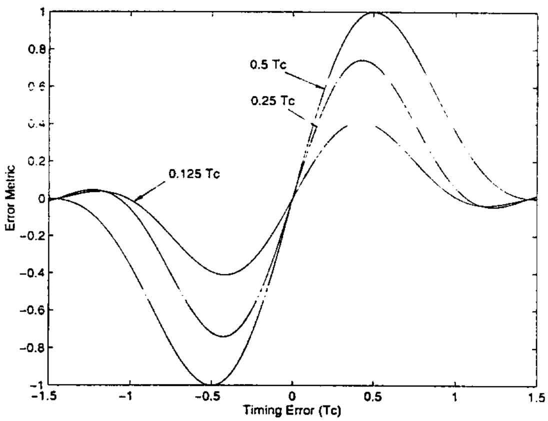

Fig. 3. S-curve for various timing offsets.

ed for various timing offsets in Fig. 3. It is seen from the figure that the pull-in range of the tracking loop is larger for the case of $\delta=0.5\ T_c$ than for the case of $\delta=0.25\ T_c$ or $0.125\ T_c$. In order to analyze the tracking performance, consider a linear equivalent model which is shown in Fig. 4. In the figure, $F(z)$ is the transfer function of the loop filter and $n(t)$ is the additive noise with variance V_o defined by Eq. (21). $K_d = N^2 E_{c,p} k$ is the phase detector gain with k denoting the slope of the S-curve at $\tau \approx 0$. Differentiating Eq. (22), we can easily obtain that k=3.242, 2.783 and 1.578 for δ=0.5, 0.25, and 0.125 T_c, respectively. From Fig. (4), the closed-loop transfer function is

$$H(z) \equiv \frac{\hat{t}(z)}{t(z)} = \frac{K_o K_d F(z) z^{-1}}{1-\{1-K_o K_d F(z)\} z^{-1}} \qquad (23)$$

Since the noise component at phase detector output can be assumed to be spectrally white, the jitter variance of the timing error is given by [10],[14]

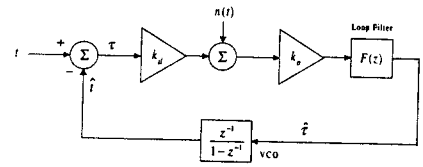

Fig. 4. Linear equivalent model.

$$\mathrm{var}(\tau) = \frac{2V_o B_L}{(N^2 E_c k)^2} \qquad (24)$$

where B_L is the loop bandwidth defined as

$$B_L = \frac{1}{2} \oint_c H(z) H\left(z^{-1}\right) \frac{dz}{j\,2\pi z} \qquad (25)$$

In the above equation, c denotes the contour integral. Using V_o *defined by Eq. (21), we can obtain jitter variance as a function of* $E_{s,p}/I_o$, pulse shaping filter, timing offset, and loop bandwidth as follow,

$$\mathrm{var}(\tau) = \frac{4\{1-R^2(2\delta)\}+8\{1-R(2\delta)\}R^2(\delta)E_{s,p}/I_o}{(E_{s,p}/I_o)^2\, k^2} B_L \qquad (26)$$

with $E_{s,p} = N E_{c,p}$.

3-3 Loop Filter Design

Most code tracking systems are second-order ones in which the first-order loop filter is employed. Therefore, we herein consider the second-order tracking loop employing type-Ⅲ loop filter with a transfer function

$$F(z) = C_1 + \frac{C_2}{1-z^{-1}} \qquad (27)$$

Inserting Eq. (27) into Eq. (23), the closed-loop transfer function can be written as

$$H(z)=\frac{K_oK_dz^{-1}\{C_1+C_2-C_1z^{-1}\}}{1-\{2-K_oK_d(C_1+C_2)z^{-1}\}+(1-C_1K_oK_d)z^{-2}}$$
$$=\frac{K_oK_dz^{-1}\{C_1+C_2-C_1z^{-1}\}}{(1-\beta_1z^{-1})\ (1-\beta_2z^{-1})} \tag{28}$$

with

$$\beta_{1,2}=\frac{2-K_oK_d(C_1+C_2)\pm\sqrt{K_oK_d\{K_oK_d(C_1+C_2)^2-4C_2\}}}{2} \tag{29}$$

Solving Eq. (25) with $H(z)$ replaced with Eq. (28), the loop bandwidth is obtained as

$$B_L=\frac{1}{2}\Big[\frac{\{\beta_1(C_1+C_2)-C_1\}\{C_1(1-\beta_1)+C_2\}}{(\beta_1-\beta_2)(1-\beta_1^2)(1-\beta_1\beta_2)}+\frac{\{\beta_1(C_1+C_2)-C_1\}\{C_1(1-\beta_2)+C_2\}}{(\beta_2-\beta_1)(1-\beta_2^2)(1-\beta_1\beta_2)}\Big] \tag{30}$$

and finally the steady-state jitter variance can be obtained by Eq. (26).

We now consider how to determine loop filter coefficients C_1 and C_2. The transient and steady-state performances of second-order tracking loops depend largely on natural frequency ω_n and damping factor ζ [11]. Given these parameters, loop filter coefficients should be determined. First consider an equivalent analog transform function which is given by

$$H(s)=H(z)\Big|_{z^{-1}=\frac{2-T_ds}{2+T_ds}}$$
$$=\frac{A+B+C}{D+E} \tag{31}$$

$$A=-\frac{K_oK_d(2C_1+C_2)}{4-K_oK_d(2C_1+C_2)}s^2$$
$$B=+\frac{K_oK_dC_1T_d}{T_d^2\{4-K_oK_d(2C_1+C_2)\}/4}s$$
$$C=+\frac{K_oK_dC_2}{T_d^2\{4-K_oK_d(2C_1+C_2)\}/4}$$
$$D=s^2+\frac{K_oK_dC_1T_d}{T_d^2\{4-K_oK_d(2C_1+C_2)\}/4}s$$
$$E=+\frac{K_oK_dC_2}{T_d^2\{4-K_oK_d(2C_1+C_2)\}/4}$$

where T_d is the timing update interval. The normalized analog transform function is given by [11]

$$H(s)\equiv\frac{2\xi\omega_ns+\omega_n^2}{s^2+2\xi\omega_ns+\omega_n^2} \tag{32}$$

Equating the denominators of Eq. (31) and Eq. (32), we can write

$$\frac{K_oK_dC_1T_d}{T_d^2\{4-K_oK_d(2C_1+C_2)\}/4}=2\xi\omega_n,$$
$$\frac{K_oK_dC_2}{T_d^2\{4-K_oK_d(2C_1+C_2)\}/4}=\omega_n^2. \tag{33}$$

Finally, we can obtain loop filter coefficients as a function of ω_n and ζ,

$$C_1=\frac{1}{K_oK_d}\frac{8\xi\omega_nT_d}{4+4\xi\omega_nT_d+(\omega_nT_d)^2},$$
$$C_2=\frac{1}{K_oK_d}\frac{4(\omega_nT_d)^2}{4+4\xi\omega_nT_d+(\omega_nT_d)^2}. \tag{34}$$

Ⅳ. Performance Evaluations and Discussions

In this section, the performance evaluation of the noncoherent code tracking loop designed at baseband is made for various system parameters and is verified by computer simulations. The coherent CDMA system designed for IMT-2000 by ETRI [4] shall be used for computer simulations. Power control with step size 0.5 dB is applied for Rayleigh fading environments but not for AWGN cases. Loop delay is assumed to be two power control groups and power control error is set to be 10 %. Timing update is made every power control group corresponding to T_d=0.625 milli-seconds. Carrier frequency is set to be 2 GHz. Dual antenna diversity is assumed to be utilized at base station and Rayleigh fading signals are generated by using Jake's model[15]. For all examples, the damping factor ξ is taken to be 0.707 and K_oK_d is set to be unity. Quantization of the timing error is not applied. Fig. 5 shows theoretical performance comparison between δ=0.5 T_c and δ=0.25 T_c cases for various natural frequencies under AWGN channel environments. The loop filter coefficients, (C1, C2), are given by (0.1318, 0.0093), (0.0942, 0.0047), and (0.0682, 0.0024) each for $\omega_n T_d$ =0.1, 0.07, and 0.05. It is observed that the tracking performance for δ=0.25 T_c is slightly better than that for δ=0.5 T_c. However, as shown in Fig. 3, it should be recognized that the pull-in range is larger for δ =0.5 T_c case than that for δ=0.25 T_c case. Figs. 6 and 7 illustrate the comparison be-

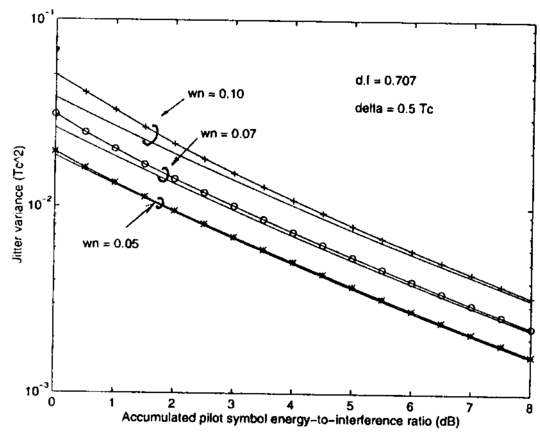

Fig. 6. Comparison between theoretical and simulation results for δ=0.5 T_c.

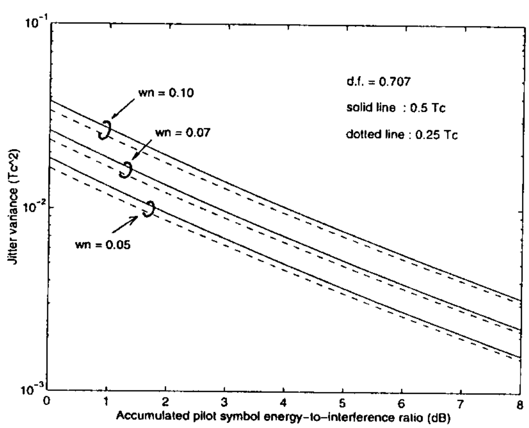

Fig. 5. Comparison of tracking performances between δ=0.5 T_c and δ=0.25 T_c cases.

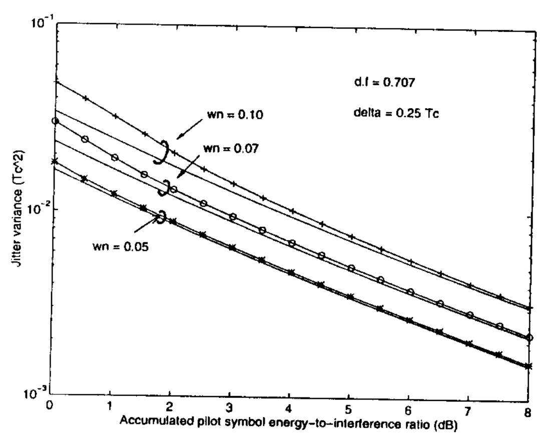

Fig. 7. Comparison between theoretical and simulation results with δ=0.25 T_c.

tween theoretical and simulation results for $\delta=0.5\ T_c$ and $0.25\ T_c$ cases, respectively, under AWGN channel environments. From the figures, we can observe that the theoretical performance is very close to the simulation result except for low $E_{s,p}/I_o$ cases. The reason why the simulation result is somewhat different from the theoretical result is simply due to the fact that the formula for steady-state jitter variance has been derived with an assumption that timing error is very small. Fig. 8 depicts code tracking performance for Rayleigh fading environments. It has been assumed that there is a single path per each antenna and the mobile speed is 100 km per hour. The normalized natural frequency $\omega_n T_d$ and timing offset δ have been selected to be 0.07 and $0.5\ T_c$, respectively. It is seen from the figure that the tracking performance in Rayleigh fading environments is degraded by about 2 dB compared with AWGN environments. It may be obvious that the tracking performance in Rayleigh fading environments shall be degraded more seriously if power control is not applied.

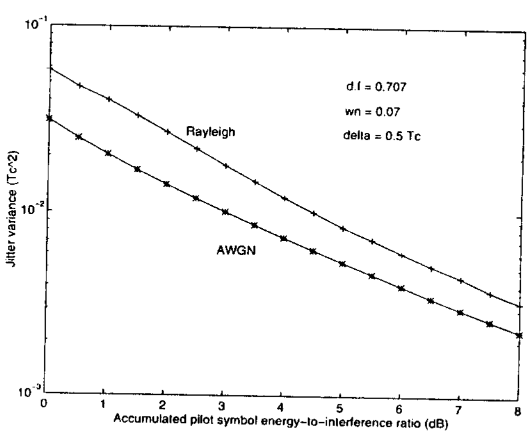

Fig. 8. Tracking performance comparison between AWGN and Rayleigh fading environments.

V. Conclusions

In this paper, analytical closed-form formula for the steady-state jitter variance of the baseband noncoherent code tracking loop designed for CDMA applications has been derived for AWGN channel environments as a function of pulse shaping filter, timing offset, signal-to-interference ratio, and loop filter coefficients. The performance evaluation of the code tracking loop has been made together with verification by computer simulations.

It has been observed that theoretical tracking performance is very close to simulation results except for low $E_{s,p}/I_o$ cases. The tracking performance for $\delta=0.25\ T_c$ is slightly better than that for $\delta=0.5\ T_c$ with a little sacrifice of the pull-in range. It has been also observed that the tracking performance in Rayleigh fading environments is degraded by about 2 dB compared with AWGN environments.

References

1. W. C. Y. Lee, "Overview of cellular CDMA," *IEEE Trans. Veh. Technol.*, vol. 40, no. 2, pp. 291-302, May 1991.
2. R. L. Pickholtz, L. B. Milstein, and D. L. Schilling, "Spread spectrum for mobile communications," *IEEE Trans. Veh. Technol.*, vol. 40, no. 2, pp. 313-322, May 1991.
3. K. S. Gilhousen, I. M. Jacobs, R. Padovani, A. J. Viterbi, L. A. Weaver, and C. E. Wheatly, "On the capacity of a

cellular CDMA system," *IEEE Trans. Veh. Technol.*, vol. 40, no. 2, pp. 303-312, May 1991.
4. S. C. Bang, H. R. Park, and Y. N. Han, "Performance analysis of a wideband CDMA system for FPLMTS," *Proc. of VTC* '97, Phoenix, pp. 830-834, May 4-7, 1997.
5. M. K. Simon, "Noncoherent pseudonoise code tracking performance of spread spectrum receivers," *IEEE Trans. Commun.*, vol. COM-25, no. 3, pp. 327-345, Mar. 1977.
6. R. A. Yost, "A modified PN code tracking loop : its performance analysis and comparative evaluation," *IEEE Trans. Commun.*, vol. COM-30, no. 5, pp. 1027-1036, May 1982.
7. B. Y. Chung, C. Chien, H. Samueli, and R. Jain, "Performance analysis of an all digital BPSK direct-sequence spreadspectrum IF receiver architecture, " *IEEE J. Selec. Areas Commun.*, vol. 11, no. 7, pp. 1096-1107, Sept. 1993.
8. M. K. Simon, J. K. Omura, R. A. Scholtz, and B. K. Levitt, *Spread spectrum communications*, vol. Ⅲ, Ch. 1, 1985.
9. H. R. Park and B. J. Kang, "On the performance of a maximum-likelihood code acquisition technique for preamble search in CDMA reverse link," To be published in *IEEE Trans. Veh. Technol.*, Nov. 1997.
10. A. J. Viterbi, CDMA : *Principles of spread spectrum communication*, Ch. 2-4, Addison-Wesley, 1995.
11. F. M. Gardner, *Phaselock technique*, John Wiley & Sons, 1979.
12. A. Papoulis, *Probability, random variables, and stochastic processes*, Ch. 7, McGrawHill, 1989.
13. A. D. Whalen, *Detection of signals in noise*, Ch. 4, Academic Press, 1971.
14. R. E. Ziemer and R. L. Peterson, *Digital communications and spread spectrum systems*, Ch. 9, Macmillan, 1989.
15. W. C. Jakes jr., *Microwave mobile communications*, Ch. 1, John Wiley & Sons, 1974.

이 경 준

1974년 : 한양대학교 전자공학과(공학사)
1982년 : 연세대학교 산업대학원 전기전자공학과(공학석사)
1994년 현재 : 한국항공대학교 대학원 전자공학과(박사과정)
1997년 현재 : 한국전자통신연구원 책임연구원(이동통신망연구부장)
[주관심 분야] 디지털 신호처리, 스마트 안테나, 이동통신 네트워크 등.

박 형 래

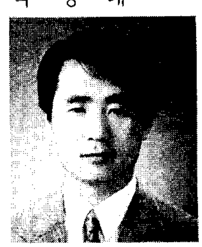

1982년 : 한국항공대학교 전자공학과(공학사)
1985년 : 연세대학교 전자공학과(공학석사)
1993년 : 미국 Syracuse Univ. 전기공학과(공학박사)
1985년~현재 : 한국전자통신연구원 책임연구원(신호기술연구실장)
[주관심분야] 신호처리, CDMA시스템 설계, 레이다 신호처리 등.

채 수 환

1973년 : 한국항공대학교 전자공학과(공학사)
1985년 : 미국 앨라배마 대학교 전자계산학과(공학석사)
1988년 : 미국 앨라배마 대학교 전자계산학과(공학박사)
1977년~1983년 : 금성통신연구원
1989년~현재 : 한국항공대학교 컴퓨터공학과 부교수
[주관심 분야] 병렬처리, 분산시스템